Calculation of radiation damage induced by neutrons in compound materials

L. Lunéville, David Simeone, C. Jouanne

Available online at www.sciencedirect.com
SCIENCE DIRECT®
Journal of Nuclear Materials 353 (2006) 89–100
journal of nuclear materials
www.elsevier.com/locate/jnucmat

Calculation of radiation damage induced by neutrons in compound materials

L. Lunéville [a], D. Simeone [b,*], C. Jouanne [a]

[a] Laboratoire d'Etudes de Protection et de Probabilités, CEA/Saclay, F-91191 Gif sur Yvette, France
[b] Laboratoire d'Analyse Microstructurale des Matériaux, CEA/Saclay, F-91191 Gif sur Yvette, France

Received 18 July 2005; accepted 2 March 2006

Abstract

Many years have been devoted to study the behaviour of solids submitted to impinging particles like ions or neutrons. The nuclear evaluations describe more and more accurately the various neutron–atom interactions. Anisotropic neutron–atom cross-sections are now available for many elements. Moreover, clear mathematical formalism now allows to calculate the number of displacements per atom in polyatomic targets in a realistic way using the binary collision approximation (BCA) framework. Even if these calculations do not take into account relaxation processes at the end of the displacement spike, they can be used to compare damages induced by different facilities like pressurized water reactors (PWR), fast breeder reactors (FBR), high temperature reactors (HTR) and fusion facilities like the European Spallation Source (ESS) and the International Fusion Material Irradiation Facility (IFMIF) on a defined material. In this paper, a formalism is presented to describe the neutron–atom cross-section and primary recoil spectra taking into account the anisotropy of nuclear reactions extracted from nuclear evaluations. Such a formalism permitted to compute displacement per atom production rate, primary and weighted recoil spectra within the BCA. The multigroup approximation has been used to calculate displacement per atom production rate and recoil spectra for a define nuclear reactor. All these informations are useful to compare recoil spectra and displacement per atom production rate produced by particle accelerator and nuclear reactor.

PACS: 61.80.Az; 61.72.Bb

1. Introduction

Submitted to irradiation by energetic particles such as ions or neutrons, atoms are displaced from their equilibrium positions in a crystal. These displaced atoms drastically increase the concentration of point defects in the crystal. The material is then driven by irradiation in a metastable thermodynamic state that can be very different from its thermodynamical equilibrium state [1]. The over-concentration of defects induced by irradiation is responsible for important structural modifications of the solid. There are many cases of interest where

* Corresponding author. Tel.: +33 1 69 08 29 20; fax: +33 1 69 08 90 82.
E-mail address: david.simeone@cea.fr (D. Simeone).

0022-3115/$ - see front matter © 2006 Elsevier B.V. All rights reserved.
doi:10.1016/j.jnucmat.2006.03.006

alloys or ceramics are maintained in such a nonequilibrium thermodynamic state by irradiation. Typical examples are provided by solids exposed to neutron irradiation in nuclear reactors. The structural stability and then the physical properties of such driven materials are largely modified. It is now well known that the kinetic evolution of defects, which is ultimately responsible for irradiation changes in material properties, is controlled by the irradiation temperature and the defect production rate [1]. This defect production rate is linked to elementary physical mechanisms associated to neutrons impinging solids [2] in nuclear reactors. This calculation incorporates, at least, to a first approximation, the impact of neutrons on material at the atomic scale. During neutron–atom collisions, a large amount of neutrons kinetic energy is transferred to atoms of the target. These recoils produce inside the crystal an important amount of defects during their slowing down. To estimate the defect production rate produced by neutrons and recoils, the dpa production rate can be calculated. One of the most useful way to estimate the defect production rate is to estimate at least the displacement per atom production rate [3].

The general topic of ion irradiation as a surrogate for neutron damage irradiation has been the topic of numerous conferences and research over the past 30 years [4–8]. As particle accelerators can induce damage in solids over a large range of incident particles fluxes and temperatures, without activation of materials, they are efficient tools to test different physical models able to describe the behaviour of materials in nuclear plants. Therefore, the nature and the energy of incident particles produced by accelerators need to be chosen in order to produce radiation damages similar to those produced in nuclear reactors. To reach such a goal, it is important to calculate and then to compare the primary and weighted recoil spectra as well as dpa production rate due to neutron–atom collisions [9,10] in nuclear reactors and ion–atom collisions in particle accelerators. The primary recoil spectrum can be exactly calculated from basic physical principles and measured neutron cross-sections for all neutron–atom interactions. Moreover, the number of displacements produced by recoil atom is also a key parameter to compare the behaviour of materials under irradiation [3]. Therefore, such calculations, leading to the calculation of the weighted recoil spectrum, require some models to describe in a more realistic way, the effects of recoils on a solid. The simplest way to calculate the weighted recoil spectra and dpa production rate in solids is to use the binary collision approximation (BCA) [11]. Therefore, it is now clearly admitted that the BCA overestimates defects in solids because the atomic relaxation of atoms in the displacement cascades is not taken into account. The correct description of displacement cascades implies in fact a description of interatomic forces in defined solids to handle the relaxation processes. The molecular dynamics technique is now extensively used to describe these relaxation phases in the displacement cascades for metals and alloys [12]. However, even if the molecular dynamics seems to be a useful tool to compute primary damage in solids, it is not possible, until now, to simulate the impact of neutrons on a defined solid. Moreover, the use of such a technique is more doubtful for ceramics because the inelastic energy loss and the dynamical charge of different ions are not taken into account [13].

In this work, a formalism describing neutron–atoms interactions is presented in detail. This formalism is used to calculate the dpa production rate and the primary and weighted recoil spectra produced in a nuclear reactor. The comparison of these spectra computed for nuclear reactors and particle accelerators allows to define the nature of particles able, in an accelerator, to simulate the evolution of solids irradiated by neutrons. These estimators have also been calculated for different facilities and for different ceramics which can be potential candidates for structural materials of the new generation of nuclear reactors.

2. Description of the formalism

When a neutron impacts on an atom, recoils are created and generate damages. The neutron–atom interaction processes are numerous [14,15] and create various types of recoil atoms of different energies. So, an accurate description of the neutron–atom interactions, i.e. elastic scattering, inelastic diffusion and charged particles emission, is essential to obtain a precise determination of recoil energies. The isotropic emission compound nucleus model (IECN) is usually used to estimate the energy of recoil atoms [16,17]. Within the IECN theory framework, particles emitted by the inelastic collisions and nuclear reactions are isotropically distributed in space. Therefore, the important anisotropy of emitted particles modifies drastically the energy distribution of recoil atoms [14,18,19]. For instance,

the evaporation model used in the IECN model does not accurately calculate the energy distribution of emitted particles during nuclear reactions [15,17]. New nuclear evaluations [20,21] give now information about the spectral and angular distribution of emitted particles.

On the other hand, the determination of the number of displacements per atom generated by atoms can be obtained thanks to numerical simulations. Therefore, the use of Monte-Carlo programs like SRIM [11] to compute the dpa production rate induced by neutrons within the BCA framework is time consuming. As the variance associated to the dpa profile is roughly inversely proportional to the square root of the number of shoots, few minutes are necessary to obtain accurate dpa profiles. Within these simulations, such a calculation must be performed for each recoil energy associated to a define neutron–atom interaction. Because a fine energy sampling (about 100 points) is needed to describe a neutron–atom interaction, a long time is necessary to compute the dpa production rate and recoil spectra. At last, analytical approximations like the Norgett Robinson and Torrens [22,23] approximation (NRT) are not accurate enough to calculate dpa in polyatomic solids such as ceramics [24–26]. These two points lead us to use the classical formalism defined by Lindhard [27] to calculate dpa for polyatomic solids. Within the Lindhard's theory framework, few seconds are needed to compute dpa versus recoil energy. With this calculation, the dpa production rate and recoil spectra can then be computed in few minutes for a fission reactor.

2.1. The neutron–atom interactions

The treatment of neutron–atom interactions needs a mathematical description of interactions [15] like elastic scattering (n,n), inelastic scattering (n,n'), charged particle emission such as (n,p), (n,d), (n,t), (n,α), $(n,{}^3He)$ and multiple particle emission such as $(n,2n)$. In such reactions, the energy of recoil atoms, T, depends on the angle θ between the incident and emitted particles, the energy of the incident particle E and, the energy of the emitted particle E' in the laboratory frame (Fig. 1). Defining μ as the cosine of θ, the cross-section describing the neutron–atom interaction is written as

$$\sigma(\mu,E,E') = \sigma(E) f(\mu,E,E')/2\pi, \tag{1}$$

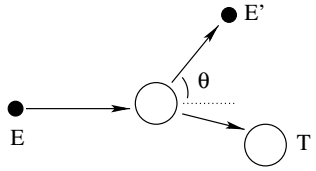

Fig. 1. Schematic description of the interaction between an incident particle (for instance a neutron) and a target atom. E is the incident particle energy, E' is the emitted particle energy, T is the recoil atom energy and θ is the angle between the incident particle direction and the emitted particle direction in the laboratory frame.

where $\sigma(E)$ is the reaction cross-section and characterizes the intensity of the interaction and $f(\mu,E,E')$ is the normalized distribution function which defines the angular and energetic spectrum of the emitted particles. Such a function describes the spatial anisotropy of the considered interaction. The neutron–atom differential cross-section $\chi(E,T)$ can be written as

$$\begin{aligned}\chi(E,T) &= \sigma(E)K(E,T)\\ &= \sigma(E)\int_0^{+\infty} \mathrm{d}E' \frac{f(\mu,E,E')}{2\pi} \frac{1}{\left|\frac{\partial T(\mu,E,E')}{\partial \mu}\right|}.\end{aligned} \tag{2}$$

The normalized distribution function $f(\mu,E,E')$, which describes the anisotropy of the interaction, appears explicitly in the definition of the PKA differential cross-section $\chi(E,T)$.

Fig. 2 presents the comparison between $K(E,T)$ for the neutron-^{58}Ni inelastic diffusion calculated taking into account the anisotropy of the reaction and within the IECN model framework [16] for 10 and 14 MeV neutron. For 14 MeV neutrons, the anisotropy of this interaction induces a spread of the energy of recoil atoms below the energy broadening estimated by the IECN model. Such a broadening of the recoil energy modifies the shape of recoil spectra and then dpa production rate.

Even if such a treatment of the inelastic interactions induces minor improvement in the calculation of $\chi(E,T)$ and then the determination of dpa production rate and recoil spectra for nuclear fission reactors, this correction is important for fusion facilities like the European Spallation Source (ESS) and the International Fusion Material Irradiation Facility (IFMIF).

For multiple particle emission reactions, proper conservation laws for the momentum and kinetic energy are used to derive mathematical relations between T, E, E' and μ (cf. Appendix A). Fig. 3

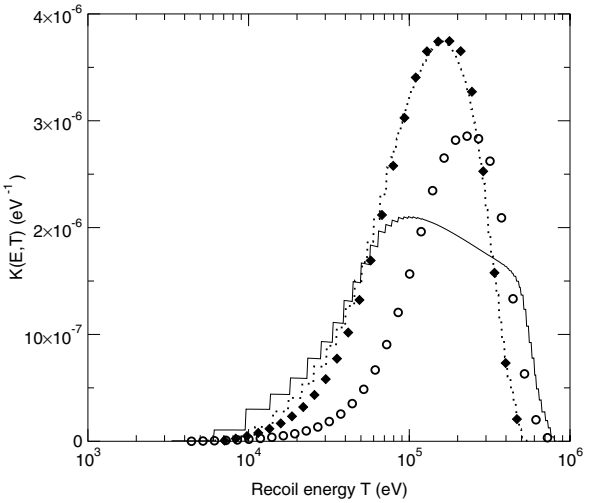

Fig. 2. Comparison of normalized differential cross-sections $K(E,T)$ associated to neutron ^{58}Ni inelastic continuum interaction computed taking into account anisotropy and within the IECN model framework. For 10 MeV neutrons, the IECN model (black diamonds) and the anisotropic model (dotted line) give similar results. For 14 MeV neutrons, the anisotropy of the reaction (line) becomes important and induces drastic changes of $K(E,T)$ compared to its valuation extracted from the IECN model (circles).

shows the comparison between $K(E,T)$ versus the α particle energy, T, calculated according to the IECN model (dashed line) and to the formalism presented in this paper (full line) for the ^{6}Li(n,t)He reaction. The mean value of the recoil energy and the shape of the two functions are very different. The gaussian-like shape of the normalized function calculated from the IECN model is replaced by a window function in the formalism presented here. The shape and the range of the recoil energy associated to this window function agrees quite well with measured and simulated values [28].

The detailed analysis of the shape of $\chi(E,T)$ for inelastic scattering and multiple particle emission reactions then shows that the formalism presented is able to describe more efficiently than the IECN model these interactions. Damage produced in absorbing materials or in particular ceramics such as B_4C, HfB_2 and $LiAlO_2$ can then be efficiently computed in fission nuclear reactors.

2.2. The calculation of the damage production within the BCA framework

To estimate the number of displaced atoms generated by incident particles in a medium, a model describing the multiple collisions between incident particles and recoils inside a solid must be introduced.

The BCA formalism is able to describe damage induced by the slowing down of particles inside a material as long as the mean free path of the moving particles remains larger than the characteristic length in the solid. The BCA breaks down for particles with mean free paths of the same order

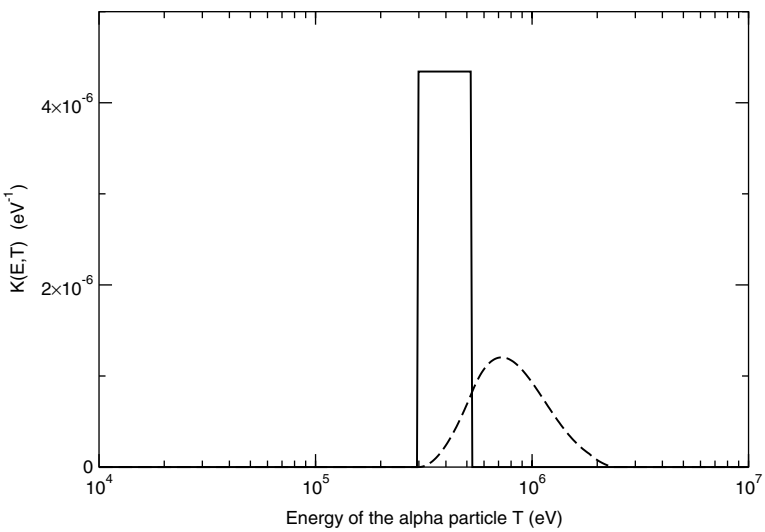

Fig. 3. Comparison of different functions $K(E,T)$ computed taking into account anisotropy (solid line) and within the IECN model framework (dashed line) associated to the ^{6}Li(n,t)He nuclear reaction induced by a 0.1 MeV neutron. Depending on the model used to describe the nuclear reaction, the energy of emitted particles are very different.

of magnitude than this characteristic length. In this case, the number of displaced atoms computed within this formalism overestimates the real amount of defects produced by irradiation. Therefore, such a formalism requires only a description of interatomic potentials accurate at distances less than equilibrium distances in a defined solid. As the screening of nuclear charges is not negligible in the velocity regime considered here, the Thomas Fermi statistical model for Coulomb potential describes accurately this interaction. The main interest of such a model is to treat all atoms as identical aside from scaling factors. Following the seminal work of Lindhard on the subject [29,30], an universal cross-section function derived from the Thomas Fermi potential describes the interaction cross-section between an incident particle and an atom of the medium. As collisions can be considered as binary encounters, the sample size is always much larger than the particles mean free path. Neglecting the crystal state of the material, a one-dimensional integral equation [30], is able to handle the evolution of energetic particles in the medium. In a polyatomic target composed of p elements, within the BCA framework [24,25], $(p+1)$ integro-differential equations allow to define the number of displacements per atom ν_{ij} versus the energy E:

$$S_j(E)\frac{\mathrm{d}\nu_{ij}(E)}{\mathrm{d}E} = c_j \int_{Ed_j}^{\lambda_{ij}E} \chi_{ij}^*(E,T)R_{ij}(T)\,\mathrm{d}T + \sum_{l=1}^{p} c_l \int_{Ed_l}^{\lambda_{il}E} \chi_{il}^*(E,T)\nu_{lj}(T)\,\mathrm{d}T, \quad (3)$$

where ν_{ij} is the number of displacements of atoms j generated by atoms of type i, $S_j(E)$ is the nuclear and electronic stopping power, c_j is the atomic concentration of the atom j, Ed_j is the displacement threshold associated to atom j, $\lambda_{ij}E$ is the maximum energy transferable in a head collision between the atoms i and j, $\chi_{ij}^*(E)$ is the elastic differential cross-section between atoms i and j. This differential cross-section is obtained from the Lindhard's universal cross-section. R_{ij} is a probability function describing the replacement of an atom i by an atom j. The interest of such a formalism, compared to the classical NRT formula, is that displacement threshold energies associated to each sublattice are correctly taken into account, i.e. subthreshold displacements can be computed [26]. The displacement threshold energy values used in this paper are extracted from previous works [31] and presented in Table 1.

Fig. 4 presents the number of displaced atoms in $ZnAl_2O_4$ as a function of Zr incident energy. The number of displaced atoms is calculated from Monte-Carlo simulations (SRIM-2003), the analytical NRT formulation and the resolution of Eq. (3). The NRT formulation always underestimates the number of displacements per atoms whereas the Lindhard's formulation slightly overestimates the number of displacements per atoms. This example justifies the use of the Lindhard's formulation for the calculation of the number of displacement per atoms for polyatomic solids.

2.3. Calculation of recoil spectra and the dpa production rate

To compare different irradiations produced by different projectiles, the primary recoil spectrum must be computed. This primary recoil spectrum is the probability distribution which describes the ability of a recoil atom to be ejected with a kinetic energy in the range $[T, T+\mathrm{d}T]$ for a defined kth interaction. The calculation of the primary recoil spectrum is achieved by the following formula:

$$\begin{aligned} Sp(E,T) &= \frac{1}{C(E)}\sum_k \int_{E_d}^{T} \chi^k(E,S)\,\mathrm{d}S \\ &= \frac{1}{C(E)}\sum_k \int_0^{+\infty} \mathrm{d}E' \\ &\quad \times \int_{\mu^k(T,E,E')}^{\mu^k(E_d,E,E')} \mathrm{d}\mu\sigma^k(\mu,E,E'), \end{aligned} \quad (4)$$

where the function $\mu^k(T,E,E')$ is the inverse function of T^k for the kth interaction (cf. Appendix A). $C(E)$ is the normalization constant associated to the primary recoil spectrum.

The primary recoil spectrum is thus able to define the averaged amount of energy transferred to recoils in a material by a given irradiation. To handle the total number of displaced atoms, a model of displacement per atom must be introduced. The elementary interactions between projectiles and atoms must then be weighted by a defined number of displacement per atoms. A more realistic comparison of different kinds of irradiation can then be obtained from the calculation of the weighted recoil spectrum. This spectrum is expressed as

Table 1
Values of displacement threshold energies of different elements of solids studied in this work

Element	C	Zr	Si	Al	O	Zn	Ti	Ni	Nb	Li
E_d (eV)	31	40	25	27	30	30	40	40	40	10

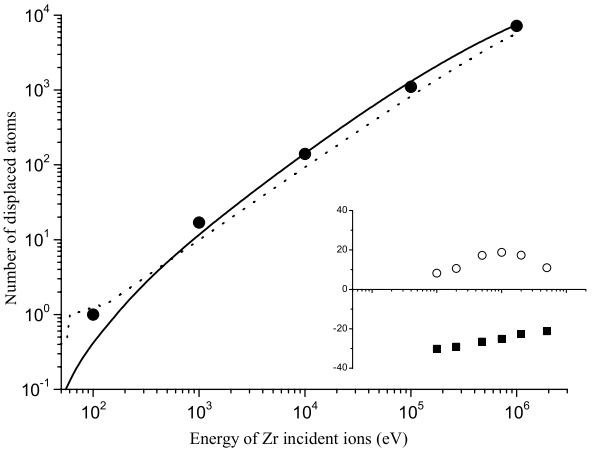

Fig. 4. Evolution of the number of displaced atoms induced by a Zr projectile in a polyatomic target the spinel $ZnAl_2O_4$. The number of displaced atoms is calculated from the SRIM-2003 Monte-Carlo program (dots), the NRT analytical formulation (dotted line) and the Lindhard's equations (full line). The insert presents the relative errors (SRIM taken as the reference) on the number of displaced atoms calculated with the NRT (black squares) and Lindhard's equation (open dots). The Lindhard's equation calculates a number of displacements closer to the one extracted from Monte-Carlo simulations.

$$W(E,T) = \frac{1}{D(E)} \sum_k \int_{E_d}^{T} \chi^k(E,S) v^k(S)\,\mathrm{d}S = \frac{1}{D(E)} \sum_k \int_0^{+\infty} \mathrm{d}E' \times \int_{\mu^k(T,E,E')}^{\mu^k(E_d,E,E')} \mathrm{d}\mu \sigma^k(\mu,E,E') v^k(T^k(\mu,E,E')), \quad (5)$$

where $\chi^k(E,T)$ characterizes the kth interaction and $v^k(T)$ is the number of displacements created by the recoil of energy T by the kth interaction and can be directly given by the resolution of Lindhard's equations. $D(E)$ is the normalization constant associated to the weighted recoil spectrum.

Whatever the nature of impinging particles, ions or neutrons, the production rate of displacements is linked to the particle flux via the total displacement per atom cross-section. Each interaction between a neutron and an atom of the medium, generates a displacement per atom cross-section. The computation of the total displacement cross-section is then achieved by summing all displacement cross-sections associated and can be computed as

$$\sigma_d(E) = \sum_k \int_0^{T_{\max}} \chi^k(E,T) v^k(T)\,\mathrm{d}T = \sum_k \int_0^{+\infty} \mathrm{d}E' \times \int_1^{\mu^k(E_d,E,E')} \mathrm{d}\mu \sigma^k(\mu,E,E') v^k(T^k(\mu,E,E')). \quad (6)$$

The energy $T_{\max}$ is the maximum energy which can be transferred to the recoil atom.

The neutron–atom cross-section $\sigma(\mu,E,E')$ is responsible for the energy distribution of recoil and then the shape of recoil spectra and the displacement cross-section. A description of neutron–atom cross-sections, taking into account anisotropic effects, allows then to compute accurate recoil spectra and dpa production rate.

3. Calculation of the damage functions

To compare the damage induced in a material by different nuclear plants, the displacement cross-section and recoil spectra have to be weighted by neutron fluxes, i.e. the number of incident neutron per surface, time and energy unit. To compute the dpa production rate, the product of the differential flux, $\phi(E)$, by the displacement cross-section, $\sigma_d(E)$, must be integrated over the energy spectrum of the flux. Fig. 5 presents neutron fluxes produced in PWRs, FBRs and HTRs [32]. As the cross-sections describing nuclear interactions present very sharp resonances versus the neutron energy, the multigroup approximation is used to compute displacement cross-section and different recoil spectra taking into account neutron flux associated to a define nuclear plant.

3.1. The multigroup approximation

To describe the sharp resonances associated to particular nuclear reactions, the ponctual nuclear

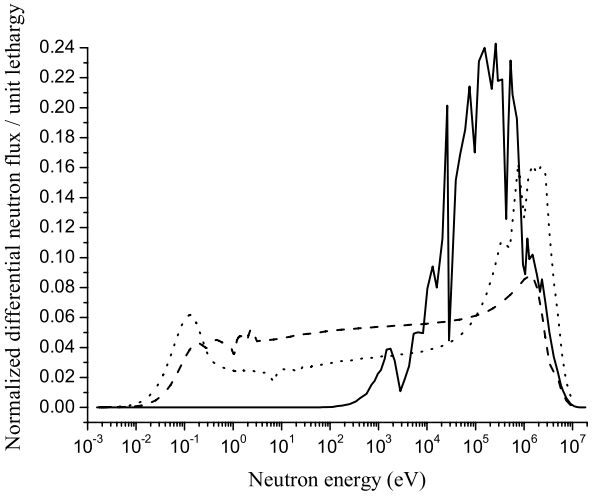

Fig. 5. Typical neutron flux spectra per lethargy unit, u ($u = \log(\frac{E}{E_0})$ where $E_0 = 1$ MeV) versus the neutron kinetic energy for three types of nuclear plants (dots for PWR, dashed line for HTR and solid line for FBR).

cross-section must be averaged. The multigroup approximation [33], allows to calculate accurate cross-sections over an important energy range with an accurate precision. The energy domain is splitted into groups ($[E_g, E_{g+1}]$). Following such a procedure, the displacement cross-section is sampled in distinct energy groups ($[E_g, E_{g+1}]$) labelled g and calculated for each group as:

$$\sigma_d^g = \frac{\int_{E_g}^{E_{g+1}} \sigma_d(E)\phi(E)\,\mathrm{d}E}{\phi_g}, \tag{7}$$

where $\phi_g = \int_{E_g}^{E_{g+1}} \phi(E)\,\mathrm{d}E$.

Integrating Eq. (6) in the group g gives:

$$\sigma_{\mathrm{d}}^g = \sum_k \int_{-1}^{1} \mathrm{d}\mu \int_0^{+\infty} \mathrm{d}E' \int_{E_g}^{E_{g+1}} \mathrm{d}E \phi(E)\sigma^k(E) \times \frac{f^k(\mu, E, E')}{2\pi} \nu^k(T^k(\mu, E, E'))/\phi_g. \tag{8}$$

Expanding the function f^k in terms of Legendre polynomials to describe the anisotropy of the reaction, gives the general formula for the total displacement cross-section:

$$\sigma_{\mathrm{d}}^g = \sum_k \sum_h \sum_{l=0}^{nl} \frac{2l+1}{2} a_{g\to h}^{l(k)} \times \int_{-1}^{1} \mathrm{d}\mu \nu^k(T^k(\mu, \overline{E_g}, \overline{E_h}))P_l(\mu) \tag{9}$$

the terms $a_{g\to h}^{l(k)}$ are the coefficients of the multigroup matrix extracted from the nuclear evaluation and averaged thanks to a multigroup procedure [34,35]. $\overline{E_g}$ is the mean energy of the group g.

In a similar way, primary and weighted spectra can be obtained following the same procedure. The dpa production rate P, becomes the sum of the total displacement cross-section multiplied by the neutron flux ϕ_g in a defined group ($P = \sum_g \sigma_g \phi_g$). These estimators integrate all informations associated to the physical nature of the solid, the description of neutron–atom interactions as well as the characteristic of the nuclear plant.

Fig. 6 illustrates the effect of the flux on recoil spectra. The total primary (left) and weighted recoil (right) spectra associated to neutron ^{93}Nb interactions have been plotted versus the recoil energy of ^{93}Nb atoms for PWR, FRB and HTR. Increasing the number of neutrons with a kinetic energy above 100 keV leads to a shift towards high kinetic energy of the primary recoil spectrum. This effect is less important for the weighted recoil spectrum as the number of displaced atoms are of the same order of magnitude for all reactors.

Fig. 7 presents the comparison of the multigroup displacement cross-section σ_g^k associated to the continuum inelastic interaction between a neutron and a ^{58}Ni atom. The full line represents the multigroup displacement cross-section obtained from Eq. (9) and the dotted line is computed from the IECN model. The anisotropy of the interaction has clearly an impact on the displacement cross-section. As expected, this impact is important for neutrons with a kinetic energy above 3 MeV in agreement with results presented in Fig. 2.

3.2. Application to ceramics

Figs. 8 and 9 show the comparison of the total multigroup displacement cross-sections as a function of the neutron energy in two polyatomic targets, SiC and $LiAlO_2$. These displacement cross-sections are calculated within the formalism developed here (solid line) and from the IECN model (SPECOMP program [31]) (dotted line). The differences between these two programs lie in the models used to estimate the number of displacements per atom and in the treatment of neutron atom interactions. Below 4 MeV, only elastic collisions occur in SiC. The use of the NRT formula in SPECOMP to calculate the number of dpa in polyatomic solids is responsible for the difference between different cross sections (cf. Fig. 8). Above 4 MeV, the anisotropy of inelastic nuclear collision is mainly responsible for the large

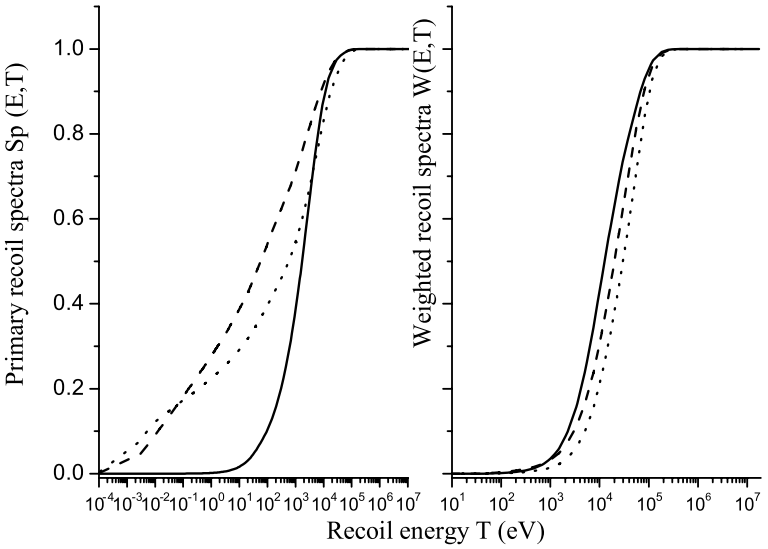

Fig. 6. Comparison of primary recoil spectra induced by 1 MeV neutron on ^{93}Nb by typical neutron fluxes produced in HTR (dashed line), PWR (dotted line) and FBR (full line). The nature of the neutron flux modifies drastically the shape of the primary recoil spectra. The weighted recoil spectra are not largely modified by the neutron fluxes.

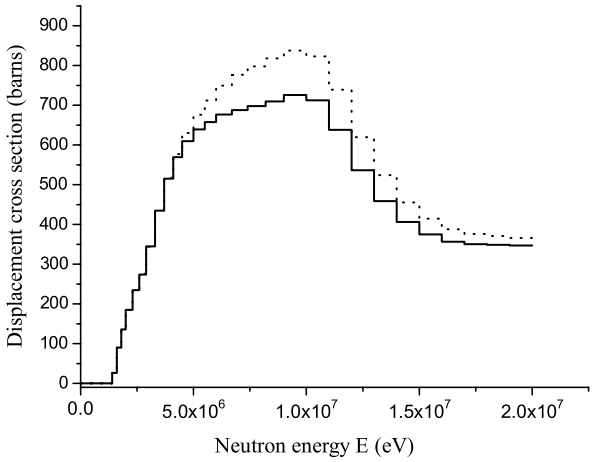

Fig. 7. Comparison of the multigroup displacement cross-section associated to the continuum inelastic interaction between neutrons and ^{58}Ni atoms. The multigroup cross-section taking into account the anisotropy (full line) and derived from the IECN model (dotted line) are plotted versus the kinetic energy of neutrons. The anisotropy of the interaction cross-section modifies drastically the multigroup displacement cross-section.

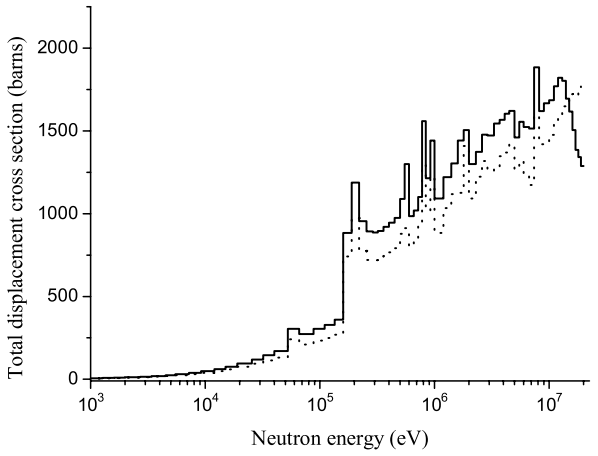

Fig. 8. Comparison of multigroup displacement cross-section computed taking into account anisotropy of nuclear reaction (full line) and within the classical IECN framework (dotted line) in SiC. The difference between two displacement cross-sections is due to the calculation of the displacements per atoms induced by recoils in this polyatomic solid below 4 MeV. Above 4 MeV, the difference between two displacement cross-sections is due to the anisotropy of the inelastic neutron–atom cross-section.

variation of displacement cross-sections. These two points are highlighted in $LiAlO_2$. Fig. 9 exhibits the impact of the neutron–atom cross-section on the displacement cross-section and then on the dpa production rate. As the ^{6}Li(n,t)He reaction is not accurately modelized in the evaporation model (cf. Fig. 3), the energy of recoil atoms is overestimated, the displacement cross-sections are then largely different over an important range of neutron energy. This effect is important in actual nuclear plants.

Three main factors control the form of displacement cross-section and recoil spectra: the displacement threshold energies, the relative atomic mass

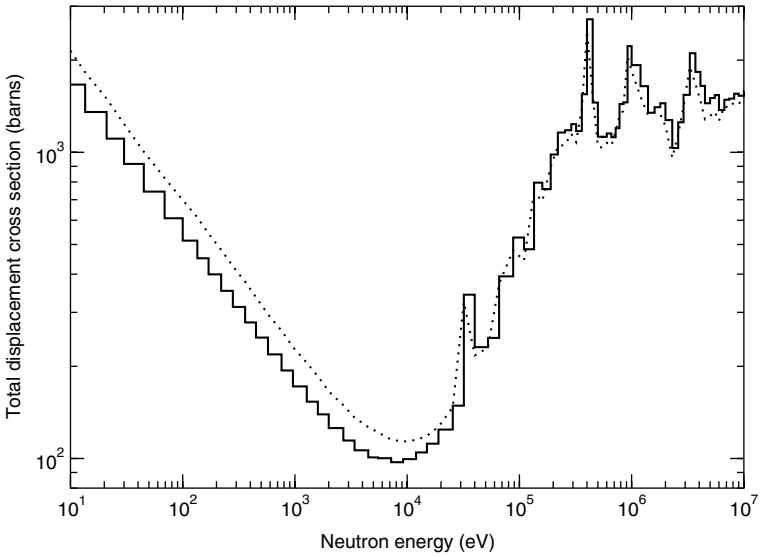

Fig. 9. Comparison of multigroup displacement cross-sections computed from the formalism developed for particle emission reaction (full line) and within the evaporation model framework (dotted line) in $LiAlO_2$. The calculated displacement cross-sections are different all over the neutron energy spectrum. The difference between the displacement cross-sections is mainly due to the different treatments of the ^{6}Li(n, t)He interaction.

and the intensity of the interaction cross-section. The shape of the recoil spectra do not vary significantly when the displacement threshold energies varies. To study the effect of the two other parameters on recoil spectra associated to a HTR facility, these spectra have been plotted for three different ceramics: ZrC, TiC and SiC (Fig. 10). As the neutron–atom cross-section of Si is quite different from those associated to Zr and Ti, it explains the shape of the primary recoil spectrum associated to SiC. The difference between ZrC and TiC primary recoil spectra is mainly due to the relative mass effect between Zr and Ti. Heavier the element, smaller the energy transfer from neutron to atom.

Fig. 11 presents displacement cross-sections versus incident particle energy calculated in order to compare radiation damage in SiC produced by HTR and particle accelerators (800 keV Bi and 150 keV Ne). The order of magnitude of these displacement cross-sections spreads over 10 decades. The dpa production rate is roughly equal to 10^{-8} dpa/s for HTR and 10^{-6} dpa/s for 800 keV Bi and 150 keV Ne irradiations with a typical flux ϕ equal to 10^{10} cm^{-2} s^{-1}. Therefore, depending on the material behaviour at the mesoscopic scale [36], these two dpa production rates may generate the same microstructural evolution of solid. Fig. 12 presents the primary recoil spectra induced by these different projectiles in SiC. The analysis of the primary

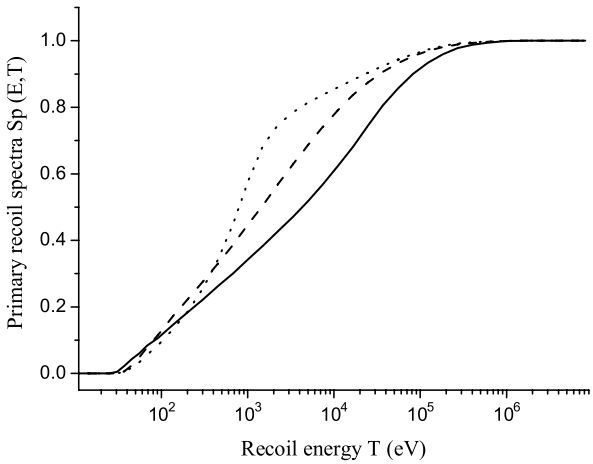

Fig. 10. Impact of the relative atomic mass and the neutron–atom cross-section on the shape of the primary recoil spectra of different materials (dots for TiC, dashed line for ZrC and full line for SiC) irradiated in an HTR.

recoil spectra clearly shows that heavy ions are not able to produce a primary recoil spectrum similar to the one produced in a HTR. However, the weighted recoil spectra induced by 800 keV Bi ions and neutrons produced in HTR are similar (Fig. 13). This analysis clearly shows that particle accelerators can at least qualitatively simulate radiation damage induced by nuclear reactors.

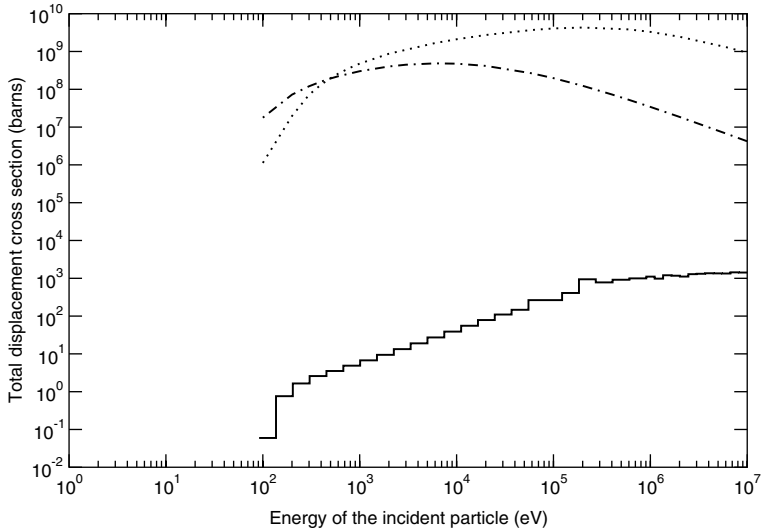

Fig. 11. Displacement cross-sections induced on SiC by 150 keV Ne (dashed-dotted line), 800 keV Bi ions (dotted line) and neutron flux of HTR (solid line).

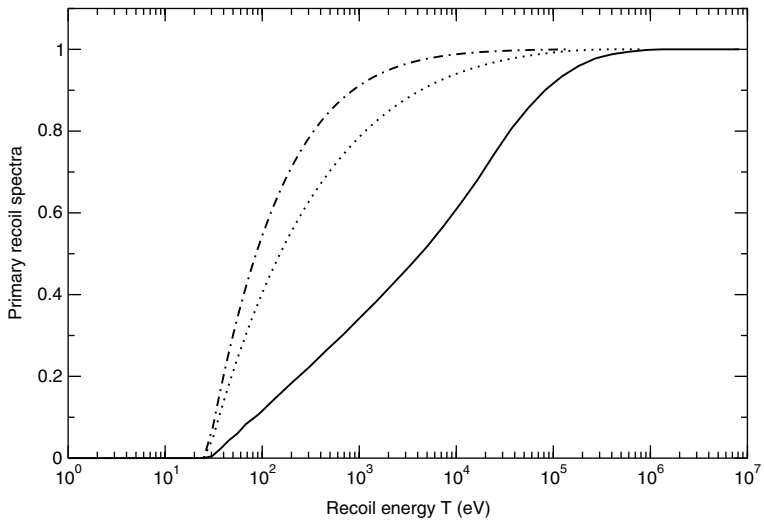

Fig. 12. Primary recoil spectra induced in SiC by 150 keV Ne (dashed-dotted line), 800 keV Bi ions (dotted line) and neutron flux of HTR (solid line). These primary recoil spectra are different.

4. Conclusion

A formalism has been introduced to describe the neutron–atom interaction taking into account information available in recent nuclear evaluations. Within this framework, the angular anisotropy of the neutron–atom interactions can easily be introduced. No models, like for instance the IECN model, are needed to compute neutron–atom cross-sections. Accurate energetic distributions of recoils produced in solids by a neutron flux, the so-called primary recoil spectra, can be calculated. Within the BCA framework, a method based on the Lindhard's works is coupled with this formalism to calculate the number of displacements per atom induced by recoils in a polyatomic target. A unique mathematical formulation permits then to calculate the weighted recoil spectrum and dpa production rate. The multigroup approximation is used to compute multigroup recoil spectra and displacement cross-section able to take into account the specific neutron flux in a defined nuclear plant. Examples of these

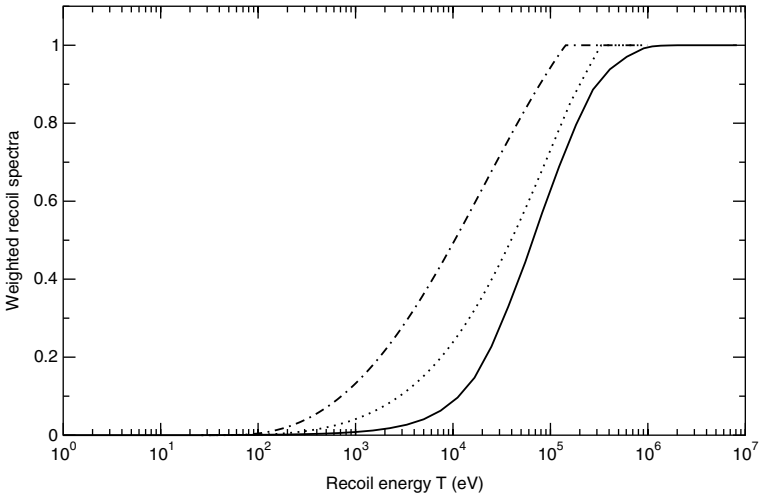

Fig. 13. Weighted recoil spectra induced on SiC by 150 keV Ne (dashed-dotted line), 800 keV Bi ions (dotted line) and neutron flux of HTR (solid line). These weighted recoil spectra are similar.

spectra have been plotted to compare the efficiency on the dpa production rate in particle accelerators and HTR in SiC. The knowledge of these spectra is a step to simulate damages due to neutrons in nuclear plant with particle accelerators.

A more precise estimation of the defect production rate can be obtained coupling the dpa obtained within the BCA frameworks with molecular dynamics simulations [37]. Work is now in progress to estimate the defect production rate in a defined solid within a more general framework [38,39].

Acknowledgements

The authors acknowledge the referee for his helpful comments and improvements of the manuscript. The authors are grateful to D. Gosset, S. Bouffard, Y. Serruys, P. Trocellier and A. Albermann for helpful comments on the manuscript. This work is supported by the CPR SMIRN program.

Appendix A. Distribution functions and recoil energy for neutron–atom interactions

A.1. Elastic scattering and discrete inelastic scattering

For these reactions, the application of kinematic laws lead to an expression for the kinetic energy T of recoils :

$$T(\mu,E,E') = \frac{1}{A+1}(E^* - 2\mu\sqrt{E^*E_a} + E_a),$$

where m_1 and m_2 are respectively the neutron and atom mass, $A = \frac{m_2}{m_1}$ is the mass ratio, Q is the energy of the reaction (0 for elastic scattering), $E^* = \frac{A+1-A'}{A+1}E$ and $E_a = Q + \frac{A}{A+1}E$ are the initial and final energies associated to the reaction in the center of mass frame.

In these reactions, recoils possess an unique energy and the spatial distribution function is

$$f(\mu,E,E') = f(\mu,E)\delta(E'-\zeta).$$

For elastic scattering, Legendre polynomials $P_l(\mu)$ are used to expand the function $f(\mu,E)$

$$f(\mu,E) = \sum_{l=0}^{nl} \frac{2l+1}{2} a^l(E) P_l(\mu),$$

where the coefficients $a^l(E)$ are obtained from the ENDFB6 nuclear evaluations.

For discrete inelastic scattering, $f(\mu,E,E')$ is directly obtained from the ENDFB6 nuclear evaluation.

A.2. Continuum inelastic scattering and (n,2n) interaction

The conservation of momentum and kinetic energy leads to the following equation for T

$$T(\mu,E,E') = \frac{1}{A}(E - 2\mu\sqrt{EE'} + E').$$

The function $f(\mu,E,E')$ is directly obtained from nuclear evaluation.

A.3. Charged particle emission

For charged particle emissions (reactions: (n, p), (n, d), (n, t), (n, α), (n, ^{3}He)), two approximations are used for the spectrum of the emitted particle. Emitted particles possess an unique energy and are uniformly distributed in space. The distribution function is thus reduced to

$$f(\mu, E, E') = \frac{1}{2}\delta(E' - \phi)$$

and the recoil energy is

$$T(\mu, E, E') = \frac{1}{A+1}(E^* - 2\mu\sqrt{A'E^*E_a} + A'E_a),$$

where A' is equal to the mass ratio of the ejected particle over the incident particle and E_a is the Coulomb energy barrier.

References

[1] G. Martin, P. Bellon, Solid State Phys. 50 (1997) 189.
[2] E. Balanzat, S. Bouffard, Materials under Irradiation, Trans Tech. Publication, 1993.
[3] R. Averback, T. Diaz de la Rubbia, Solid State Phys. 50 (1997) 189.
[4] A revue of these works can be found in C. Abromeit, J. Nucl. Mater. 216 (1994) 78.
[5] M. Bleiberg, J. Benne (Eds.), International Conference on Radiation Effects in Breeder Reactor Structural Materials, Scottsdale, AIME, New York, 1977.
[6] H. Brager, J. Perrin (Eds.), International Conference on Effects of Radiation on Materials, Scottsdale, ASTM, Philadelphia, 1982.
[7] F. Garner, N. Packan, A. Kumar (Eds.), International Conference on Radiation Induced Changes in Microstructure, Seattle, ASTM, Philadelphia, 1986.
[8] See also J. Nucl. Mater. 85&86 (1979).;
J. Nucl. Mater. 103&104 (1983).;
J. Nucl. Mater. 122&123 (1984).;
J. Nucl. Mater. 141–143 (1986).;
J. Nucl. Mater. 179–181 (1991).;
J. Nucl. Mater. 191&192 (1993).
[9] R. Averback, J. Nucl. Mater. 33 (1971) 108.
[10] R. Averback, R. Benedeck, K. Merkle, Phys. Rev. B 18 (1978) 4156.
[11] J. Ziegler, J. Biersack, U. Littmark, The Stopping Power and Range of Ions in Solids, Pergamon, 1985.
[12] D. Bacon, T. Diaz de la Rubbia, J. Nucl. Mater. 216 (1994) 275.
[13] Y. Limoge, A. Barbu, Defects Diffus. Forum 237–240 (2004) 621.
[14] W. Meyerhoff, Elements of Nuclear Physics, Dunod, 1970.
[15] K. Kikuchi, M. Kawai, Nuclear Matter and Nuclear Reactions, North Holland Publishing, 1968.
[16] See for instance the compilation of L. Greenwood, J. Nucl. Mater. 206 (1994) 25.
[17] G. Odette, D. Doiron, Nucl. Technol. 29 (1976) 346.
[18] D. Olander, Fundamental Aspect of Nuclear Reactor Fuel elements, Energy research and Development Administration TI-26711-PI, Library of Congress, 1976.
[19] M. Walt, H. Barschall, Phys. Rev. 1062 (1954) 93.
[20] V. MacLane, ENDF-102 data formats and procedures for the evaluated nuclear data file ENDF-6, Cross Section Evaluation Working Group, BNL-NCS-44945-02/04-Rev, 2001.
[21] The JEFF3.0 Nuclear Data Library, JEFF Report 19, NEA, OCDE, 2000.
[22] M. Norgett, M. Robinson, I. Torrens, An Analytical Way to Compute DPA in Solids, CEA-Report CEA-R-4389, 1972.
[23] M. Norgett, M. Robinson, I. Torrens, Nucl. Eng. Des. 33 (1975) 50.
[24] D. Parker, C. Coulter, J. Nucl. Mater. 101 (1981) 261.
[25] A. Albermann, D. Lesueur, Am. Soc. Testing Mater. 19 (1989) 19103.
[26] D. Simeone, O. Hablot, V. Micalet, P. Bellon, Y. Serruys, J. Nucl. Mater. 246 (1998) 206.
[27] J. Lindhard, V. Nielsen, M. Schraff, Kgl. Dan. Vid. Mat. Fys. Medd. 36 (1968) 1.
[28] F. Mann, Hauser*5, A computer code to calculate nuclear cross sections, HEDL-TME-78-83, 1979.
[29] J. Lindhard, Phys. Rev. B 14 (1961) 1.
[30] J. Lindhard, V. Nielsen, M. Schraff, P. Thomsen, Kgl. Dan. Vid. Mat. Fys. Medd. 10 (1963) 33.
[31] L. Greenwood, R. Smither, SPECTER: Neutron Damage Calculation For Materials Irradiations, ANL/FPP/TM-187, 1985.
[32] X. Raepsaet, private communication.
[33] J. Bussac, P. Reuss, Traité de neutronique, Hermann, 1978.
[34] R. MacFarlane, D. Muir, The NJOY Nuclear Data Processing System, LA-12740-M, Los Alamos, 1999.
[35] R. MacFarlane, D. Muir, F. Mann, J. Nucl. Mater. 122 (1984) 1041.
[36] J. Roussel, P. Bellon, Phys. Rev. B 65 (2002) 144107.
[37] S. Jumel, J. Van Duysen, J. Nucl. Mater. 328 (2004) 151.
[38] Y. Cheng, M. Nicolet, W. Johnson, Phys. Rev. Lett. 58 (1987) 2083.
[39] Y. Cheng, Mater. Sci. Rep. 5 (1990) 45.